Degradation and physical properties of sugar palm starch/ sugar palm nanofibrillated cellulose bionanocomposite

Article *in* Polimery -Warsaw- · August 2019

DOI: 10.14314/polimery.2019.10.5

CITATIONS
3

READS
181

9 authors, including:

Atikah Mahamud
Universiti Putra Malaysia
13 PUBLICATIONS **98** CITATIONS
SEE PROFILE

Ilyas R.A.
Universiti Putra Malaysia
67 PUBLICATIONS **693** CITATIONS
SEE PROFILE

S. M. Sapuan
Universiti Putra Malaysia
803 PUBLICATIONS **11,531** CITATIONS
SEE PROFILE

Mohamad Ridzwan Ishak
Universiti Putra Malaysia
155 PUBLICATIONS **2,208** CITATIONS
SEE PROFILE

Degradation and physical properties of sugar palm starch/ sugar palm nanofibrillated cellulose bionanocomposite

M.S.N. Atikah[1)], R.A. Ilyas[2), 3)], S.M. Sapuan[2), 3), *)], M.R. Ishak[4)], E.S. Zainudin[3)], R. Ibrahim[5)], A. Atiqah[6)], M.N.M. Ansari[6)], R. Jumaidin[7)]

DOI: dx.doi.org/10.14314/polimery.2019.10.5

Abstract: This paper aims to study the degradation rate of sugar palm nanofibrillated cellulose (SPNFCs) and sugar palm starch (SPS). SPNFCs were isolated from sugar palm fiber, while SPS is extracted from sugar palm trunk. The SPNFCs were reinforced with SPS biopolymer as biodegradable reinforcement materials of different diameter/length based on the number of passes of high pressurize homogenization process (5, 10 and 15 passes represented by SPS/SPNFCs-5, SPS/SPNFCs-10, and SPS/SPNFCs-15). These SPNFCs were incorporated into SPS plasticized with glycerol and sorbitol *via* solution casting method. Soil burial experiment performed on SPS and SPS/SPNFCs bionanocomposites showed that SPS was degraded more rapidly by losing 85.76% of its mass in 9 days compared to 69.89% by SPS/SPNFCs-15 bionanocomposite. The high compatibility between SPNFCs nanofiber and SPS biopolymer matrices can be observed through field emission scanning electron microscopy (FE-SEM).

Keywords: sugar palm, high pressurized homogenizer, nanofibrillated cellulose, nanocomposites, soil burial degradation.

Degradacja i właściwości fizyczne bionanokompozytów skrobi palmy cukrowej wzmocnionej nanowłóknami celulozowymi tej palmy

Streszczenie: Zbadano szybkość degradacji nanowłóknistej celulozy wyizolowanej z palmy cukrowej (*Arenga pinnata*) (SPNFCs) oraz skrobi wydzielonej przez ekstrakcję z rdzenia pnia tej palmy (SPS). SPNFCs uzyskiwano z włókien palmy cukrowej, poddawanych homogenizacji pod wysokim ciśnieniem w 5, 10 lub 15 cyklach, otrzymując nanowłókna celulozy o różnej długości i średnicy. SPNFCs wprowadzano do SPS uplastycznionego mieszaniną (1 : 1) glicerolu i sorbitolu. Metodą odlewania z roztworu wytwarzano błony nanokompozytowe SPS/SPNFCs-5, SPS/SPNFCs-10 i SPS/SPNFCs-15. Test glebowy procesu biodegradacji wykazał, że SPS ulegało szybszej degradacji, tracąc 85,76% swojej masy w ciągu 9 dni, w porównaniu z ubytkiem masy 69,89% w wypadku bionanokompozytu SPS/SPNFCs-15. Na podstawie analizy metodą skaningowej mikroskopii elektronowej z emisją polową (FE-SEM) stwierdzono dużą kompatybilność między nanowłóknami SPNFCs i biopolimerową osnową SPS.

Słowa kluczowe: palma cukrowa, homogenizacja wysokociśnieniowa, nanowłóknista celuloza, nanokompozyty, degradacja w glebie.

Nowadays, total biodegradable green composite or biocomposite, which are made up of natural matrices and natural fibers, have attracted many researchers for the advantages they offer. The major factors contributing to the increase of interest include the rise in petroleum prices and the inevitable environmental pollution contrib-

[1)] Universiti Putra Malaysia, Department of Chemical and Environmental Engineering, 43400 UPM Serdang, Selangor, Malaysia.

[2)] Universiti Putra Malaysia, Institute of Tropical Forestry and Forest Products, Laboratory of Biocomposite Technology, 43400 UPM Serdang, Selangor, Malaysia.

[3)] Universiti Putra Malaysia, Department of Mechanical and Manufacturing Engineering, 432400 UPM Serdang, Selangor, Malaysia.

[4)] Universiti Putra Malaysia, Department of Aerospace Engineering, 43400 UPM Serdang, Selangor, Malaysia.

[5)] Forest Research Institute Malaysia, Pulp and Paper Branch, 52109 Kepong, Selangor, Malaysia.

[6)] Universiti Tenaga Nasional, Institute of Power Engineering, 43000 Kajang, Selangor, Malaysia.

[7)] Universiti Teknikal Malaysia Melaka, Fakulti Teknologi Kejuruteraan Mekanikal dan Pembuatan, Hang Tuah Jaya, 76100 Durian Tunggal, Melaka, Malaysia.

[*)] Author for correspondence; e-mail: sapuan@upm.edu.my

uted by non-biodegradable petroleum-based polymeric materials [1, 2]. Among various types of renewable polymers, starch is one of the most widely used and favorable materials for biodegradable plastic due to its low cost and high availability [3–5]. In the last decade, the thermoplastic starch, or plastic starch (PS), has gained attention and offered an attractive alternative to petroleum-based polymers when long-term biodegradation is unnecessary and rapid degradation is needed [6, 7]. However, plastic starch biopolymer still exhibits some drawbacks, such as poor mechanical properties and high hydrophilic nature. PS biopolymers have limited use as starch-based films in the packaging applications compared to the conventional synthetic polymers that are currently being used, known as thermoplastics. Thus, to overcome these problems, various chemical and physical treatments have been employed, including blending PS with other synthetic polymers, chemical modification, graft copolymerization, and incorporating fillers, such as lignin, cellulose and nanocellulose and fibers (*i.e.* sugar palm fiber) [6–9].

Sugar palm is a multipurpose tree propagated in South Asia to Southeast Asia; from Taiwan to Philippines, Indonesia, Papua New Guinea, India, North Australia, Malaysia, Thailand, Burma, and Vietnam [10–12]. It is considered as a potential source for natural fibers and biopolymer. The main component of sugar palm fibers (SPF) structure is cellulose (66.5%), which leads to their outstanding mechanical properties. Another attractive potential of sugar palm is the ability to produce biopolymers (*i.e.* starch) [13]. The starch obtained from the trunks of sugar palm trees can be used as a feedstock in biodegradable polymer manufacturing, which can be reinforced with natural fibers to make biodegradable composites. This composite owns the advantage of being easily available, inexpensive, renewable source, and most importantly biodegradable [13–15].

Nonetheless, the tensile strength of SPF is constrained due to its complex structure and the inevitable imperfections of the cell wall, which resulted from the processing steps or inherent from growth. Therefore, significant improvements can be achieved with nanofibrillated cellulose (NFCs), which can be extracted from various natural fibers, especially SPF, due to their high aspect ratio, high Young's modulus, and high bending strength. NFCs can be extracted from high pressurize homogenization (HPH) process. HPH is known as one of the eco-friendly methods due to its efficiency and simplicity and does not require any organic solvents during the process. HPH process involves passing the cellulose slurry through a very small nozzle at high pressure energy to break the cellulose slurry to the smallest possible size of the fibers from micro to nanoscale [16]. Recently, the application of NFCs as a load-bearing constituent in the development of novel and low-cost biodegradable materials has been raised [17–20]. The development of the nanocomposite from sugar palm starch (SPS) and sugar palm nanofibrillated cellulose (SPNFCs) may be the expected solution to overcome this problem.

SPS/SPNFC bionanocomposites can potentially be applied as packaging material. Therefore, in order to study the durability of bionanocomposites, their physical and degradation properties must be thoroughly determined.

Fig. 1. Sugar palm fiber wrapped around the tree trunk from top to bottom

So far, to the best of our knowledge, no study on the biodegradation characteristic of SPNFCs (5, 10 and 15 passes) reinforced SPS biopolymer composites had been reported in the literature. Therefore, in this study, nanofibrillated cellulose (NFCs) from sugar palm fibers was extracted by using high pressurized homogenization treatment at various passes (5, 10 and 15 passes). Then, the as-prepared NFCs were incorporated into the SPS matrix for the preparation of nanocomposite materials. Nanocomposites were obtained using solution casting method with NFCs and gelatinized starch solution at constant weight ratios of NFCs with different passes. Nanocomposite film structure and biodegradation properties were investigated by using field emission scanning electron microscopy (FE-SEM), physical tests, and biodegradability tests. These basic data are necessary for the design and use of the resultant bionanocomposites.

EXPERIMENTAL PART

Materials

Sugar palm fibers (SPFs) and sugar palm starch (SPS) (Table 1) were obtained from sugar palm trees at Jempol, Negeri Sembilan (Malaysia). Plasticizers, such as sodium hydroxide, sodium chlorite, acetic acid, sorbitol (Table 2) and glycerol (Table 3) were provided by Sue Evergreen Sdn Bhd (Semenyih, Malaysia).

Preparation of SPNFCs

Sugar palm fibers (SPFs) were extracted from different parts of the sugar palm trees (sugar palm frond, trunks, and bunches). The sugar palm fibers are readily wrapped around the tree trunk of the tree from top to bottom (Fig. 1). SPF was removed from the tree using a knife. In order to gain uniform SPF size (2 mm), grinding and screening process was done by using a Fritsch pulverisette mill. The procedure for the cellulose preparation was reported elsewhere [21]. The extraction of sugar palm cellulose (SPC) from SPF was carried out *via* two main processes: delignification and mercerization, both were performed in accordance with ASTM D1104-56 (1978) and ASTM D1103-60 (1977) for the removal of lignin and hemicellulose, respectively.

SPNFCs were prepared from SPC *via* mechanical treatment [22]. The refining process of sugar palm cellulose (SPC) was performed according to ISO 5264-2:2002 for 20,000 passes in a PFI-mill. Then, the obtained fibers were isolated *via* the process of high pressurized homogenization (HPH). Fibers suspension (1.8%) was processed in a high pressurized homogenizer (GEA Niro Soavi, Panda NS1001L, Parma, Italy) at 50 MPa for 5, 10 and 15 passes. This process broke down the fibers from macro-sized to nano-sized structures, forming slurries of nanofibrillated cellulose. The SPNFCs suspensions were then freeze-dried at -110 °C in ethylene gas medium to get nanofibrillated powder.

T a b l e 1. Sugar palm starch specification

Properties	Specification
Density, g/cm^3	1.54
Ash, %	0.20
Amylose, %	37.60
Protein, %	0.10
Fat, %	0.27
Water content, %	15.00

T a b l e 2. Sorbitol specification

Properties	Specification
Assay, % (HPLC)	> 99.0
Heavy metals, % (as Pb)	< 0.001
Mannitol, % (HPLC)	< 0.2
Water, %	< 0.2

T a b l e 3. Glycerol specification

Properties	Specification
Assay, %	99.8
Density 20/4°, g/cm^3	1.257–1.262
Refractive index	1.471–1.473
pH	6.0–7.0
Sulphate ash, %	Max. 0.005
Chloride (Cl), %	Max 0.0001
Sulphate (SO_4), %	Max 0.0005
Ammonium (NH_4), %	Max 0.0005
Arsenic (As), %	Max 0.0004
Copper (Cu), %	Max 0.0005
Iron (Fe), %	Max 0.0005
Lead (Pb)	Max 0.0005
Sugar (glucose), %	Max 0.0004

Preparation of the SPS/SPNFCs bionanocomposite films

The plasticizer sugar palm starch/sugar palm nanofibrillated celluloses (SPS/SPNFCs) composite film was produced using solution casting method. A mixture of starch, sorbitol, glycerol, SPNFCs and distilled water were mixed and sonicated together to obtain homogenous nanocomposite film [21]. SPNFCs solution was prepared *via* mixing and sonicating process with 190 cm^3 of distilled water with a known concentration of SPNFCs (0.5 wt % on the starch basis of 10 g) and were added to the SPS film-forming mixture and stirred at 1000 rpm for 20 min in a disperser. After that, 30 wt % of combined glycerol and sorbitol (at 1 : 1 glycerol to sorbitol ratio) as a single plasticizer was added to the mixture under constant stirring (100 rpm) while the mixture was heated at 95 °C for 20 minutes at 85 °C in a disperser to gelatinize the starch. The ratio of plasticizer was fixed for all samples. The plasticizers are used to improve the processability and flexibility of starch biopolymer by reducing the strong intermolecular inter-

actions between starch molecules. Then, the film-forming suspension was left to cool down and was placed under vacuum to remove air bubbles inside it prior to casting by putting 45 g of the suspension into petri dishes sized of 15 cm diameter. The petri dishes containing the film-forming solution were placed in an oven at 40 °C overnight. SPS films were prepared without SPNFCs served as the control (designed as SPS film), whereas the nanocomposite film with different passes of 5, 10 and 15 times was denoted as SPS/SPNFCs-5, SPS/SPNFCs-10, and SPS/SPNFCs-15, respectively. The resulting films were kept in the desiccator at room temperature for a week to ensure the equilibrium of the water content in the films prior to any characterization tests.

Methods of testing

Transmission electron microscopy (TEM)

High-resolution transmission electron microscopy (Hitachi H-7100, Tokyo, Japan) was used to determine the diameter size of SPNFCs. A drop of SPNFCs solution was placed on the copper grid surface. Later, uranyl acetate was used to stain the sample to improve the contrast. The sample was left for 1 minute to dry at room temperature for better observation and contrast image during TEM analysis.

Field emission scanning electron microscopy (FE-SEM)

Field emission scanning electron microscope (FEI NOVA NanoSEM 230, Brno-Černovice, Czech Republic) was used to observe the surface of the nanocomposite films before and after the biodegradability test. To avoid any charging during the FE-SEM analysis, all the films were coated with gold using argon plasma metallizer (sputter coater K575X, Crawley, United Kingdom) [22, 23].

X-ray diffraction (XRD)

The X-ray diffraction patterns of SPNFCs was done by using Rigaku D/max 2500 X-ray powder diffractometer (Rigaku, Tokyo, Japan) equipped with CuKα radiation (λ = 0.1541 nm) in the 2θ range 10–40°. The crystallinity index of each fiber sample X_c, as depicted in Eq. (1) can be deduced from the empirical method reported by Segal *et al.* [24].

$$X_c = \frac{(I_{002} - I_{am})}{I_{002}} \cdot 100\% \quad (1)$$

where: I_{002}, I_{am} – the peak intensities of crystalline and amorphous materials, respectively.

Density

The density of the control bio-based films and nanocomposite biopolymer films was measured using an electronic densimeter (Mettler-Toledo (M) Sdn. Bhd, 11106706). Xylene was used as the immersing liquid instead of distilled water to avoid water uptake by the hydrophilic film samples. Films were placed into desiccators containing P_2O_5 that act as drying agent. Initially, the films were weighed (m, [g]). After that, the film was immersed in xylene solution. The volume of xylene (v, [cm^3]) before and after putting the film was recorded (V [cm^3] is the film volume). The density (ϱ) of the film was calculated according to Eq. (2) [25]. The test was repeated for 6 times.

$$\varrho = \frac{m}{V} \quad (2)$$

Film thickness

Biopolymer films thickness was determined by using digital micrometer (digimatic micrometer, Mitutoyo Japan, Series 293 MDC-MX Lite). Six random measurements were taken at 27 °C and the average value was calculated for each type of samples.

Biodegradability test

Biodegradability test was conducted to measure the weight loss of control biopolymer films and nanocomposites films after they were buried in a soil for a certain time. The biopolymer films with a size of 3 × 1 cm were buried into the soil with a depth of 10 cm beneath the soil surface [1, 6, 26, 27]. After 24, 48, 72, 168, 216, and 264 h, the samples were dug out, washed with distilled water and weighed. Then, the samples were placed into the vacuum oven at 40 ºC overnight. The weight loss (%) of the films were calculated according to Eq. (3). Where, w_0 (initial weight of sample), w_t = (weight after a certain time in soil). The test was repeated for 3 times.

$$Weight\ loss(\%) = \frac{W_0 - W_t}{W_0} \cdot 100\% \quad (3)$$

Statistical analysis

In order to accomplish the analysis of variance (ANOVA) on the obtained data and to conduct means comparisons at a 0.05 level of significance ($p \leq 0.05$), SPSS software and Tukey's Test was used.

RESULTS AND DISCUSSION

Physical properties of sugar palm nanofibrillated cellulose (SPNFCs)

The physical properties of the SPNFCs from different treatments were determined using Image J software. The images were obtained from the TEM analysis. Figures 2 and 3 show the TEM micrograph and physical properties (length and diameter) of the SPNFCs, respectively. TEM micrograph of SPNFCs in Fig. 2 revealed the nanometric dimension. Figure 3 illustrated the average length of

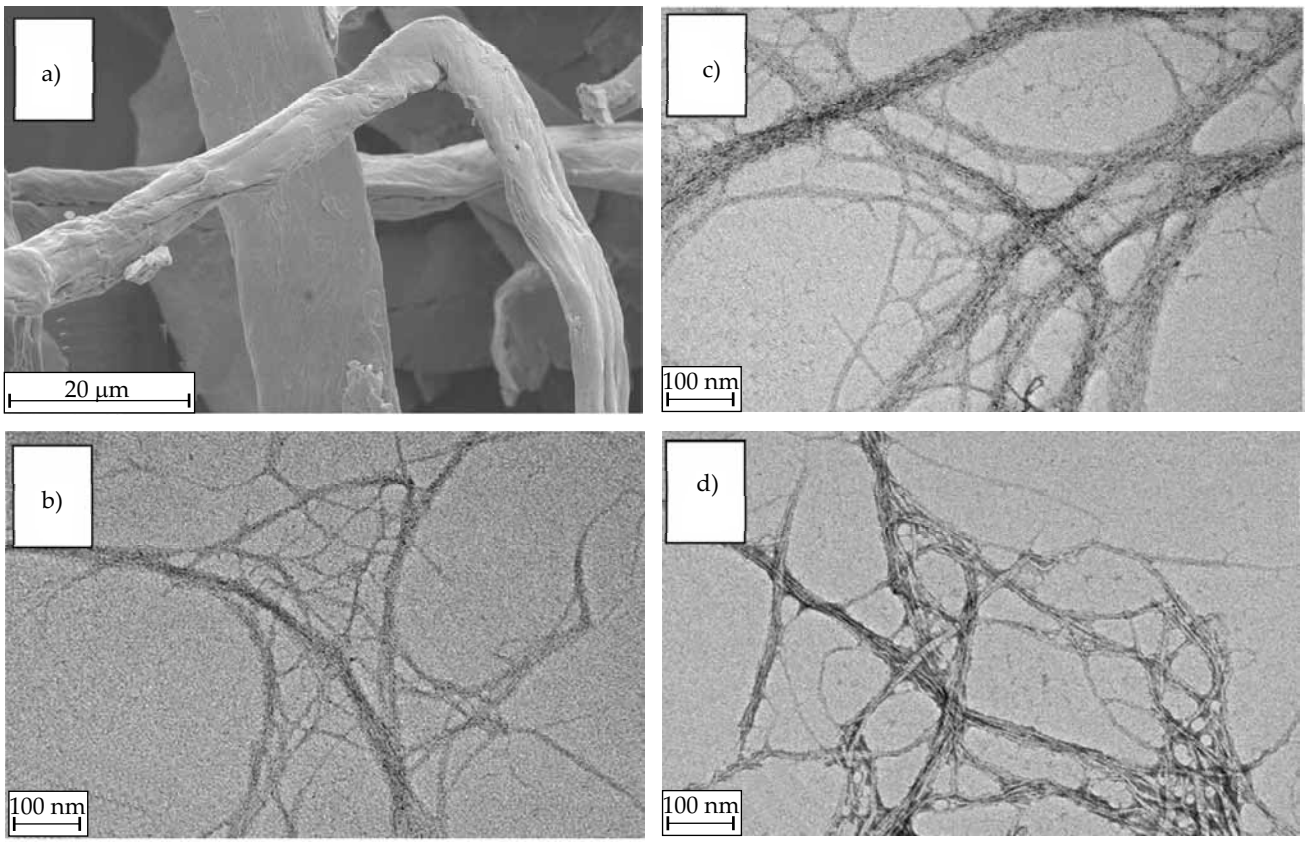

Fig. 2. a) FE-SEM micrographs of the SPC and TEM micrographs of: b) the SPNFCs-5, c) SPNFCs-10, d) SPNFCs-15

SPNFCs-5, SPNFCs-10 and SPNFCs-15 and their diameter. The diameters measured were similar to the diameters of structures of nanocellulose that were obtained from other agrowaste sources, such as banana (5 nm) [28], and flax fiber (5 nm) [29, wider than prickly pear fruit (2–5 nm) [30], and smaller than *Alfa tenassissima* (5–20 nm), pineapple leaf (30 nm) [31], sugarcane bagasse (35 nm) [32], wheat straw (30–70 nm) [33], hemp fiber (10–60 nm) and rutabaga (80 nm) [29]. The resultant images in Fig. 2 revealed that the aqueous suspensions, which contained sugar palm NFCs existed mostly in the form of individual crystals and some formed aggregates.

In addition, the reduction of the diameter of the SPNFCs-5 (2615.2 nm) compared to SPC (11.87 μm) was 99.8%. This might be contributed by high shearing force that broke down the physical cohesion of the aggregated fibrils, which consequently initiated the release of microfibrils into individualized nanofibers after HPH process [34]. The defibrillation of SPNFCs process was then continued for SPNFCs-10 and SPNFCs-15. The changes in the diameter size of the SPNFCs were observed, which were reduced by 46% and 74% for SPNFCs-10 and SPNFCs-15, respectively, compared to SPNFCs-5. Figure 3 also shows the length of SPNFCs-5, SPNFCs-10 and SPNFCs-15. The process of the high pressurized homogenization continued for the SPNFCs-10 and SPNFCs-15 for 10 and 15 passes, indicating the changes in the size of the SPNFCs which was reduced by 13% and 15% compared to SPNFCs-5, respectively. This phenomenon occurred due to the addition of the passes assisted by high impact and shear force, which defibrillated microfiber into nanofibers. Thus, the higher the number of passes, the smaller the diameter of the nanofibers.

Moreover, internal and external fibrillation during the process of HPH influenced the defibrillation process of SPNFCs. External fibrillation happens due to the harsh activities on the surface of the sugar palm fibers, whereas internal fibrillation happens by the breaking of the hydrogen bond. Both external and internal fibrillation occurred by the extended mechanical action of the high pressurize homogenization process [35]. According to

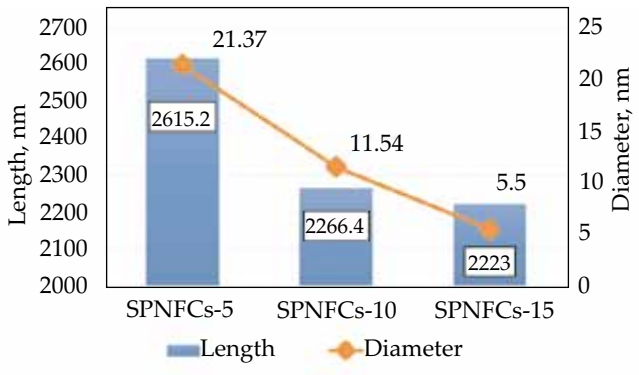

Fig. 3. Length and diameter of SPNFCs-5, SPNFCs-10 and SPNFCs-15

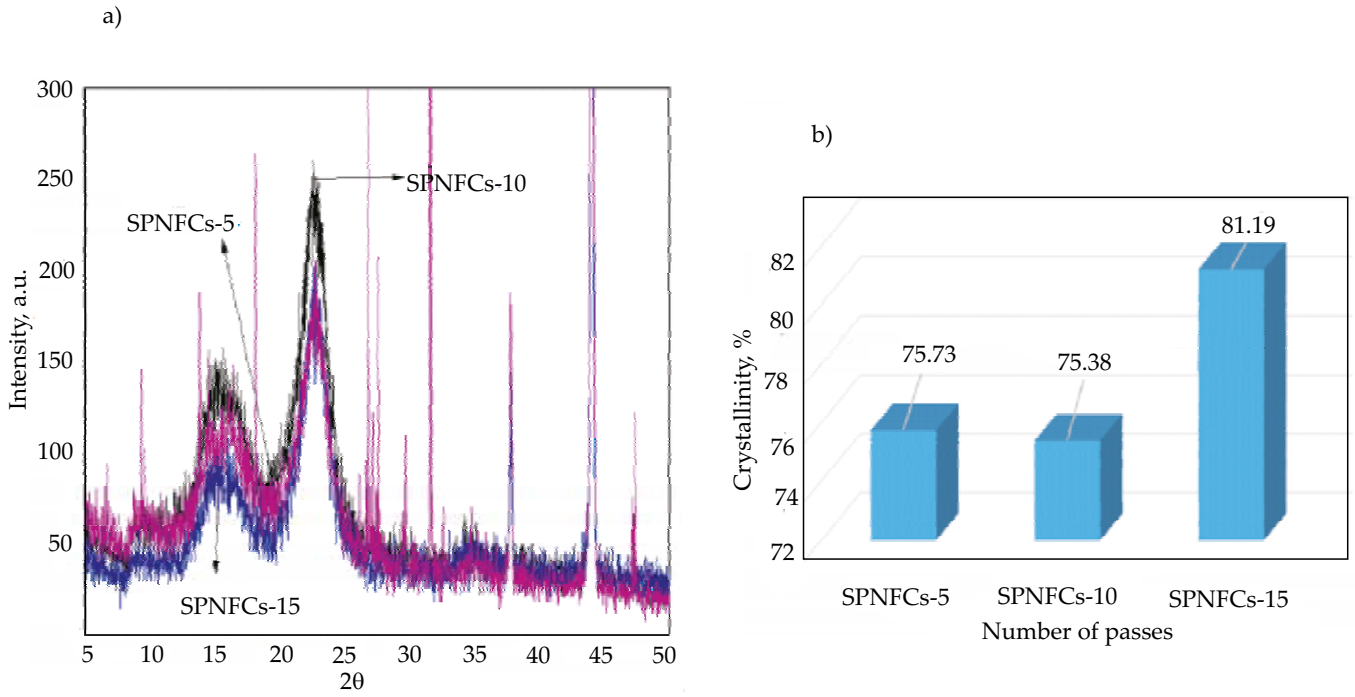

Fig. 4. a) X-ray diffraction patterns, b) crystallinity of SPNFCs-5, SPNFCs-10, and SPNFCs-15

Khalil *et al*. [35], there are several effects that might occur during the extended passes or passes of high pressurize homogenization process: (1) decreased diameter and thickness sizes of nanofibers, (2) reduction of dimension ratio (length/diameter) of nanofiber, (3) increase in the surface area of nanofiber, (4) decrease of the degree of polymerization of fiber, and (5) improvement of thermal stability and crystallinity of nanofibers. Nevertheless, according to Joonobi *et al*. [36], the physical, shape, size and morphological properties of the nanofibrillated cellulose depend on the nanocellulose and source fibers isolation process.

Figure 4 shows that the degree of crystallinity of nanofibers increased with an increase of the number of HPH passes.

The highest crystallinity index was observed for SPNFCs-15, and the lowest crystallinity index was measured for SPNFCs-10, with the values of 81.2% and 75.4%, respectively. The results showed that the crystallinity index of SPNFCs was insignificantly decreased. This might be due to the breaking of the cellulose chain, which later caused the crystal structure region between cellulose chains to collapse and become damaged during the HPH process [37]. Nevertheless, after several numbers of passes from 10 to 15 passes, the crystallinity index increased gradually. This might be due to the process of HPH that not only breaks the amorphous regions but also restructures and enriches the semi-crystalline cellulose regions [35].

Thickness and density of bionanocomposite

Table 4 shows the thickness values achieved for all samples resulted from a restricted dry mass content per unit area of the casting plate of the film-forming solutions used in the procedure. The result showed no significant difference. Furthermore, Table 4 presents a more pronounced difference in the densities of the films between control SPS and SPS/SPNFCs nanocomposite films. This is associated with the low concentrations of the filler incorporated within the film matrix, in which the SPNFCs were found to have a low density of 1.1000 ± 0.0026 g/cm^3. According to Samir *et al*. [38] and Slavutsky and Bertuzzi [25], the reinforcement of nanofibrillated cellulose had no influence on the density of poly(oxyethylene) and corn starch, respectively. However, there is a small increment in the density of the films with the addition of nanofiller SPNFCs, as shown in Table 4. The chemical and mechanical treatment caused the opening of fiber-bundles and defibrillation of individualized raw sugar palm fiber, in which indirectly decreased the size of the fiber from micro to nanoscale. This will eventually increase the interfacial spaces between the nanofibril. Higher density was found in films with a higher number of HPH passes compared to the lower ones. This phenomenon might have resulted from the chemical properties of the nanofiller, in which abundance of hydroxyl group in large surface area of SPNFCs (14.01 m^2/g) contributes to strong interactions among SPNFCs themselves that were partly destroyed during the HPH process. A new and strong interfacial adhesion was formed between SPNFCs nanofiller and SPS matrix film. The higher the HPH passes, the smaller the diameter of the nanofiber, thus, the surface area of nanofiber was increased. In addition, the formation of the strong adhesion between matrix/nanofiller had decreased the free volume inside SPS biopolymer, thus, making it denser compared to the control starch

T a b l e 4. Thickness and density of bionanocomposites

Sample	Thickness, μm	Density*), g/cm^3
SPS	123.6 ± 3.5^a	1.41 ± 0.01^a
SPS/SPNFCs-5	124.5 ± 2.1^a	1.42 ± 0.01$^{a, b}$
SPS/SPNFCs-10	124.2 ± 3.3^a	1.42 ± 0.01^b
SPS/SPNFCs-15	124.1 ± 1.3^a	1.43 ± 0.01^c

*) Values with different letters in the same column are significantly different ($p < 0.05$).

film. This decrement contributed to the increment in the density of the films.

Biodegradation of bionanocomposites

It is important to study the biodegradation properties of biocomposite films as they are closely related to the environment degradation. Biodegradation is defined as the disintegration of materials by the action of fungi, bacteria and microorganisms, or by other biological means. The speed of biodegradations process is mainly dependent on the temperature, humidity, number and type of microbes [39]. In general, the decomposition of polymer starts when these microbial organisms come into contact with the biodegradable polymer [40]. The polymer is then broken down into smaller compound, which has reduced average molecular weight through the enzymatic or metabolic process. This process, on the other hand, is also known as mineralization [41]. Figure 5 displays the mass loss curve of the SPS and SPS/SPNFCs bionanocomposites from the biodegradation test. At the end of day 7, control SPS had lost 61.9% of its original mass, whereas the SPS/SPNFCs bionanocomposite had lost 56.9%, 55.8% and 52.6% mass for SPS/SPNFCs-5, SPS/SPNFCs-10, and SPS/SPNFCs-15, respectively. The average degradation rate was found to be at 8.9%/day, 8.1%/day, 7.9%/day and 7.5%/day, respectively for the control SPS, SPS/SPNFCs-5, SPS/SPNFCs-10, and SPS/SPNFCs-15, respectively. The mass loss of SPS/SPNFCs composite observed was always lower than SPS at any given time points. This indicates that the presence of SPNFCs could disrupt the degradation of starch. The SPNFCs reinforcement within the starch composite is possible due to the strong adhesion of SPNFCs to the starch matrix phase, which decelerated the starch nanocomposite degradation by removing any formation of porous structure into a compact structure. The compatibility in both composites was resulted by the improvement of the interfacial bonding between starch matrix and nanofibers.

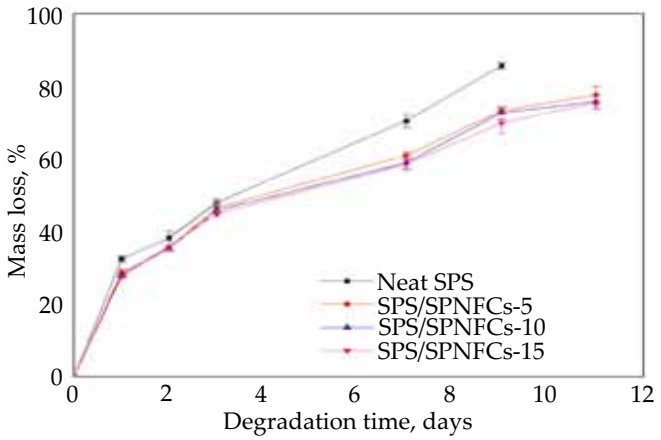

Fig. 5. Mass loss of SPS/SPNFCs nanocomposite films as a function of soil burial time

Furthermore, it can be observed that the film with higher HPH passes of nanofiller showed a slightly lower significant value of weight loss compared to the lower HPH passes of nanofiller. The higher the HPH passes, the smaller the diameter of the nanofiber, thus, the surface area of nanofiber increased. The higher the surface area, the more interfacial adhesion created between nanofiber and matrix. Moreover, the formation of strong adhesion between the matrix and nanofiller has affected the free volume inside the SPS biopolymer to reduce, thus, making it denser compared to control starch film. The SPS film was completely degraded after 10 days, while bionanocomposites films needed 14 days for complete degradation. The weight loss for the SPS film was higher than the average weight losses for all bionanocomposite films. There are two factors that might be attributed to this phenomenon to occur, which are film water absorption and degree of crystallinity of SPNFCs in bionanocomposite films [39].

Water absorption properties of the bionanocomposites were reduced due to the restricted chain mobility within the biopolymer film. The restriction was caused by the SPNFCs nanofiller which created a three-dimensional cellulosic network with the starch biopolymer [42, 43]. From Fig. 5, it can be observed that the weight loss of the bionanocomposites is lower than that of the control films. This is due to the properties of control biopolymer film, which absorbs water more than bionanocomposite films, making the films to be attacked by microorganism [44]. According to Kiatkamjornwong *et al*. [45], the growth of the microorganism occurred in the presence of sufficient moisture content. This phenomenon can be linked to the water absorption properties of starch biopolymer films. The water absorption properties of control film, SPS/ SPNFCs-5, SPS/SPNFCs-10 and SPS/SPNFCs-15 are 122.3%, 111.3%, 106.6% and 102.5% respectively. This might be ascribed to the hydrophilic behavior of the control biopolymer film [44,46]. Hence, we can summarize that the films containing smaller size of SPNFCs are resistant to biodegradation activities compared to control biopolymer films.

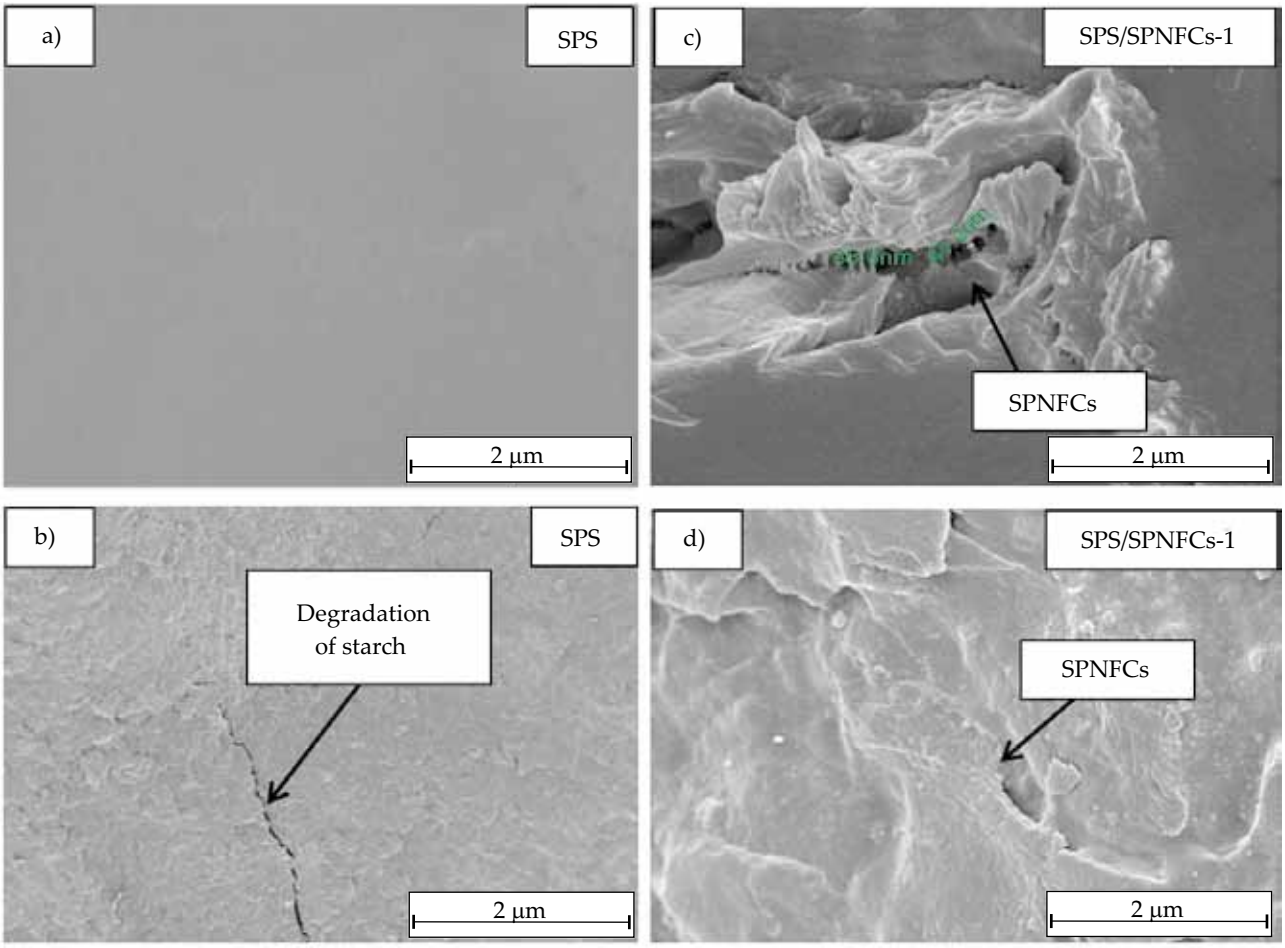

Fig. 6. Surface morphology of: a), b) control SPS film, c), d) SPF/SPNFCs-1 bionanocomposite; before (a, c) and after being buried (b, d)

Cellulose is made up of amorphous region, which is less oriented, and crystalline region, which is highly oriented. The ability of microorganism activities to degrade cellulose strongly depends on the degree of crystallinity [47]. According to Fan *et al*. [48], the major structural parameter that affects the degradation of cellulose is the degree of crystallinity of cellulose itself. These findings are supported by Alvarez *et al*. [49], where they found that the crystalline region within the cellulose component is more difficult to degrade compared to the amorphous region. SPS/SPNFCs nanocomposites were indicated to have higher crystallinity index compared to control SPS, in which this make nanocomposites to be more resistant to the microorganism compared to neat starch. This phenomenon can be proved through the mass loss of neat and nanocomposites film in Fig. 5. The microorganism attack began with the starch biopolymer then continuously to the SPNFCs. This can be seen through the variance in resistance to microbial organism attack between control and nanocomposite films. In the case of the latter, after the microorganisms attacked the surrounding starch biopolymer, the nanocomposites start to lose their structural integrity [26]. This might lead to the deterioration of mechanical properties of nanocomposites as bonding between the starch and SPNFCs weakened. Later, when all of the starch biopolymers were attacked by microorganisms, these microorganisms would then attack the SPNFCs [50, 51]. Moreover, the result obtained during the experiment showed that the control and nanocomposite films do not cause any ecological impact as it is fully degraded in the soil.

Surface morphology

The surface morphology of control and nanocomposite SPS/SPNFCs-1 film before and after being buried for 168 h in compost soil is displayed in Fig. 6. The images were generated using FE-SEM microscopy. It can be seen from the figure that most of the starch component in control and nanocomposites films had degraded. The incorporation of SPNFCs within the starch biopolymer films delayed the biodegradation of bionanocomposites. Moreover, it can be observed in Fig. 6 that the control starch biopolymer displayed a smooth and continuous surface compared with nanocomposites films. Furthermore, there are no crack and trace of starch granular found on these surfaces. These findings were also supported by Dias *et al*. [52] and Sanyang *et al*. [21], in which similar observations were made for neat rice flour films and sugar palm starch films.

However, after the film was buried in soil for 168 h, the control film surface became wavy and rough due to

the growth and microbial attacks that occurred within the soil as shown in Fig. (6b, 6d). For the SPS/SPNFCs nanocomposites surface, the evenly and highly dispersed distribution of SPNFCs can be seen in Fig. (6 c). The image shows a strong interfacial adhesion between SPNFCs and sugar palm starch biopolymer nanocomposites. According to Bilbao-Sainz *et al*. [53], the functional properties of polymer nanocomposites can be enhanced or improved by incorporating the nanofiller with well-dispersed distribution within the polymer matrix. In Fig. (6 d), the SPNFCs in the SPS/SPNFCs nanocomposites were observed to be pulled out from the starch biopolymer matrix. An excessive number of SPNFCs was seen distributed on the surface of the bionanocomposites. This phenomenon might be attributed to the microorganism activities on the film surface, which later revealed the SPNFCs images that adhere within the film. Therefore it can be summarized that natural fibers and biopolymers have attracted considerable attention of scientist and industries due to their sustainable nature and environmentally friendly [54-58].

CONCLUSIONS

Nanofibrillated cellulose with diameters of 21.37 ± 6.91 nm, 11.54 ± 2.77 nm, and 5.5 ± 0.99 nm were defibrillated from three different passes, named, SPNFCs-5, SPNFCs-10 and SPNFCs-15. Novel bionanocomposite where both natural biopolymer matrix and natural fiber derived from under-utilized parts of the sugar palm tree was successfully developed. From the study of biodegradation, it was found that the neat biopolymer SPS degraded faster in SPS/SPNFCs bionanocomposites, which lost 85.8% of its weight in 9 days compared to 69.9% by SPS/SPNFCs-15 bionanocomposite. The performance improvement of these SPS/SPNFCs bionanocomposites might be due to the high compatibility derived from intermolecular hydrogen bonding interaction between these two biomaterials as a result of their chemical similarities. In addition, good dispersion and adhesion of the SPNFCs within the SPS biopolymer matrix can be seen through FESEM micrograph. The SPNFCs established in this current work is aimed to be utilized in SPNFCs/Starch-based nanocomposites for potential packaging application.

REFERENCES

[1] Jumaidin R., Sapuan S.M., Jawaid M. *et al*.: *International Journal of Biological Macromolecules* **2017**, *97*, 606. http://dx.doi.org/10.1016/j.ijbiomac.2017.01.079

[2] Mazani N., Sapuan S.M., Sanyang M.L. *et al*.: "Lignocellulose for Future Bioeconomy" Elsevier, 2019, Chapter 15, pp. 315–332. http://dx.doi.org/10.1016/B978-0-12-816354-2.00017-7

[3] Abral H., Dalimunthe M.H., Hartono J. *et al*.: *Starch/Staerke* **2018**, *70*, 1. http://dx.doi.org/10.1002/star.201700287

[4] Asrofi M., Abral H., Kasim A. *et al*.: *Fibers* **2018**, *6*, 40. http://dx.doi.org/10.3390/fib6020040

[5] Abral H., Basri A., Muhammad F. *et al*.: *Food Hydrocolloids* **2019**, *93*, 276. http://dx.doi.org/10.1016/j.foodhyd.2019.02.012

[6] Ilyas R.A., Sapuan S.M., Ishak M.R., Zainudin E.S.: *IOP Conference Series: Materials Science and Engineering* **2018**, *368*, 012006. http://dx.doi.org/10.1088/1757-899X/368/1/012006

[7] Halimatul M.J., Sapuan S.M., Jawaid M. *et al*.: *Polimery* **2019**, *64*, 422. http://dx.doi.org/10.14314/polimery.2019.6.5

[8] Ilyas R.A., Sapuan S.M., Ishak M.R., Zainudin E.S.: *Carbohydrate Polymers* **2018**, *202*, 186. http://dx.doi.org/10.1016/j.carbpol.2018.09.002

[9] Ilyas R.A., Sapuan S.M., Ishak M.R. *et al*.: "Sugar Palm Biofibers, Biopolymers, and Biocomposites" First Edition,| Boca Raton, FL : CRC Press/Taylor & Francis Group, CRC Press, 2018, Chapter 10, pp. 189–220. http://dx.doi.org/10.1201/9780429443923-10

[10] Sapuan S.M., Ishak M.R., Leman Z. *et al*.: *INTROPica* **2017**, pp. 12–13.

[11] Ilyas R.A., Ammar I.M., Sapuan S.M. *et al*.: " Sugar Palm Biofibers, Biopolymers, and Biocomposites" First Edition, Boca Raton, FL : CRC Press/Taylor & Francis Group, CRC Press, 2018, Chapter 12, pp. 246–264. http://dx.doi.org/10.1201/9780429443923-12

[12] Sapuan S.M., Ilyas R.A.: *INTROPica* **2017**, pp. 5–7.

[13] Sanyang M.L., Ilyas R.A., Sapuan S.M., Jumaidin R.: "Bionanocomposites for Packaging Applications", Cham: Springer International Publishing, 2018, pp. 125–147. http://dx.doi.org/10.1007/978-3-319-67319-6_7

[14] Radzi A.M., Sapuan S.M., Jawaid M., Mansor M.R.: *Fibers and Polymers* **2017**, *18*, 1353. http://dx.doi.org/10.1007/s12221-017-7311-8

[15] Ilyas R.A., Sapuan S.M., Sanyang M.L. *et al*.: *Current Analytical Chemistry* **2018**, *14*, 203. http://dx.doi.org/10.2174/1573411013666171003155624

[16] Ilyas R.A., Sapuan S.M., Ibrahim R. *et al*.: *Journal of Materials Research and Technology* **2019**. http://dx.doi.org/10.1016/j.jmrt.2019.04.011

[17] Megashah L.N., Ariffin H., Zakaria M.R., Hassan M.A.: *IOP Conference Series: Materials Science and Engineering* **2018**, *368*, 012049. http://dx.doi.org/10.1088/1757-899X/368/1/012049

[18] Megashah L.N., Ariffin H., Zakaria M.R., Ando Y.: *IOP Conference Series: Materials Science and Engineering* **2018**, *368*, 012001. http://dx.doi.org/10.1088/1757-899X/368/1/012001

[19] Kian L.K., Jawaid M., Ariffin H., Alothman O.Y.: *International Journal of Biological Macromolecules* **2017**, *103*, 931. http://dx.doi.org/10.1016/j.ijbiomac.2017.05.135

[20] Sabaruddin F.A., Paridah M.T.: *IOP Conference Series: Materials Science and Engineering* **2018**, *368*, 012039.

http://dx.doi.org/10.1088/1757-899X/368/1/012039
[21] Sanyang M.L., Sapuan S.M., Jawaid M. *et al*.: *BioResources* **2016**, *11*, 4134. http://dx.doi.org/10.15376/biores.11.2.4134-4145
[22] Ilyas R.A., Sapuan S.M., Ishak M.R., Zainudin E.S.: *BioResources* **2017**, *12*, 8734. http://dx.doi.org/10.15376/biores.12.4.8734-8754
[23] Ilyas R.A., Sapuan S.M., Ishak M.R.: *Carbohydrate Polymers* **2018**, *181*, 1038. http://dx.doi.org/10.1016/j.carbpol.2017.11.045
[24] Segal L., Creely J.J., Martin A.E., Conrad C.M.: *Textile Research Journal* **1959**, *29*, 786. http://dx.doi.org/10.1177/004051755902901003
[25] Slavutsky A.M., Bertuzzi M.A.: *Carbohydrate Polymers* **2014**, *110*, 53. http://dx.doi.org/10.1016/j.carbpol.2014.03.049
[26] Sahari J., Salit M.S., Zainudin E.S., Maleque M.A.: *Fibers and Textiles in Eastern Europe* **2014**, *22*, 96.
[27] Jumaidin R., Sapuan S.M., Jawaid M. *et al*.: *International Journal of Biological Macromolecules* **2017**, *99*, 265. http://dx.doi.org/10.1016/j.ijbiomac.2017.02.092
[28] Zuluaga R., Putaux J.L.L., Restrepo A. *et al*.: *Cellulose* **2007**, *14*, 585. http://dx.doi.org/10.1007/s10570-007-9118-z
[29] Bhatnagar A.: *Journal of Reinforced Plastics and Composites* **2005**, *24*, 1259. http://dx.doi.org/10.1177/0731684405049864
[30] Habibi Y., Mahrouz M., Vignon M.R.: *Food Chemistry* **2009**, *115*, 423. http://dx.doi.org/10.1016/j.foodchem.2008.12.034
[31] Balakrishnan P., Sreekala M.S., Kunaver M. *et al*.: *Carbohydrate Polymers* **2017**, *169*, 176. http://dx.doi.org/10.1016/j.carbpol.2017.04.017
[32] Mandal A., Chakrabarty D.: Carbohydrate Polymers **2011**, *86*, 1291. http://dx.doi.org/10.1016/j.carbpol.2011.06.030
[33] Kaushik A., Singh M., Verma G.: *Carbohydrate Polymers* **2010**, *82*, 337. http://dx.doi.org/10.1016/j.carbpol.2010.04.063
[34] Ilyas R.A., Sapuan S.M., Ishak M.R., Zainudin E.S.: *International Journal of Biological Macromolecules* **2019**, *123*, 379. http://dx.doi.org/10.1016/j.ijbiomac.2018.11.124
[35] Khalil H.P.S.A., Davoudpour Y., Islam M.N. *et al*.: *Carbohydrate Polymers* **2014**, *99*, 649. http://dx.doi.org/10.1016/j.carbpol.2013.08.069
[36] Jonoobi M., Oladi R., Davoudpour Y. *et al*.: *Cellulose* **2015**, *22*, 935. http://dx.doi.org/10.1007/s10570-015-0551-0
[37] Samir O.M., Madhu S., Somashekar R.: *Fibers and Polymers* **2010**, *11*, 413. http://dx.doi.org/10.1007/s12221-010-0413-1
[38] Samir A., Alloin F., Sanchez J. *et al*.: *Macromolecules* **2004**, *37*, 1386.
[39] Norazlina H., Hadi A.A., Qurni A.U. *et al*.: *IOP Conference Series: Materials Science and Engineering* **2018**, *342*, Conf. 1. http://dx.doi.org/10.1088/1757-899X/342/1/012025
[40] Edhirej A., Sapuan S.M., Jawaid M., Zahari N.I.: *Fibers and Polymers* **2017**, *18*, 162. http://dx.doi.org/10.1007/s12221-017-6251-7
[41] Youtey N.T., Bahafid W., Sayel H., El Ghachtouli N.: "Biodegradation – Life of Science" (Eds. Chamy R., Rosenkranz F.), InTech, 2013, Chapter 11, 289. http://dx.doi.org/10.5772/56194
[42] Khan A., Khan R.A., Salmieri S. *et al*.: *Carbohydrate Polymers* **2012**, *90*, 1601. http://dx.doi.org/10.1016/j.carbpol.2012.07.037
[43] Noshirvani N., Ghanbarzadeh B., Fasihi H., Almasi H.: *International Journal of Food Engineering* **2016**, *12*, 37. http://dx.doi.org/10.1515/ijfe-2015-0145
[44] Sahari J., Sapuan S.M., Zainudin E.S., Maleque M.A.: *Journal of Biobased Materials and Bioenergy* **2013**, *7*, 90. http://dx.doi.org/10.1166/jbmb.2013.1267
[45] Kiatkamjornwong S., Sonsuk M., Wittayapichet S. *et al*.: *Polymer Degradation and Stability* **1999**, *66*, 323. http://dx.doi.org/10.1016/S0141-3910(99)00082-8
[46] Halimatul M.J., Sapuan S.M., Jawaid M. *et al*.: *Polimery* **2019**, *64*, 9, 27. http://dx.doi.org/10.14314/polimery.2019.9.4
[47] Wan Y.Z., Luo H., He F. *et al*.: *Composites Science and Technology* **2009**, *69*, 1212. http://dx.doi.org/10.1016/j.compscitech.2009.02.024
[48] Fan L.T., Lee Y.H., Beardmore D.H.: *Biotechnology and Bioengineering* **1980**, *22*, 177. http://dx.doi.org/10.1002/bit.260220113
[49] Alvarez V.A., Ruseckaite R.A., Vázquez A.: *Polymer Degradation and Stability* **2006**, *91*, 3156. http://dx.doi.org/10.1016/j.polymdegradstab.2006.07.011
[50] Żuchowska D., Steller R., Meissner W.: *Polymer Degradation and Stability* **1998**, *60*, 471. http://dx.doi.org/10.1016/S0141-3910(97)00110-9
[51] Ilyas R.A., Sapuan S.M., Ishak M.R., Zainudin .ES.: Journal of Advanced Research in Fluid Mechanics and Thermal Sciences **2018**, *51*, 234.
[52] Dias A.B., Müller C.M.O., Larotonda F.D.S., Laurindo J.B.: *LWT – Food Science and Technology* **2011**, *44*, 535. http://dx.doi.org/10.1016/j.lwt.2010.07.006
[53] Bilbao-Sainz C., Bras J., Williams T. *et al*.: *Carbohydrate Polymers* **2011**, *86*, 1549. http://dx.doi.org/10.1016/j.carbpol.2011.06.060
[54] El-Shekeil Y.A., Sapuan S.M., Khalina A. *et al.: Express Polymer Letters* **2012**, 6, 1032. http://dx.doi.org/0.3144/expresspolymlett.2012.108
[55] Mansor M.R., Sapuan S.M., Zainudin E.S. *et al.: Materials & Design* **2014**, 54, 473. http://dx.doi.org/10.1016/j.matdes.2013.08.064
[56] Razali N., Salit M.S., Jawaid M. *et al.:* BioResources, **2015**, 10, 1, 1803. http://dx.doi.org/10.15376/biores.10.1.1803-1824
[57] Ilyas R.A., Sapuan S.M., Ishak M.R. *et al.:* "6th Postgraduate Seminar on Natural Fiber Reinforced Polymer Composites", Serdang 2018, pp. 55–59.

Received 13 III 2019.